Particle swarm optimised fuzzy controller for charging–discharging and scheduling of battery energy storage system in MG applications

M. Faisal [a], M.A. Hannan [a,*], Pin J. Ker [a], M.S.Abd. Rahman [a], R.A. Begum [b], T.M.I. Mahlia [c]

[a] *Department of Electrical Power Engineering, Universiti Tenaga Nasional, 43000 Kajang, Malaysia*
[b] *Institute of Climate Change, Universiti Kebangsaan Malaysia, 43600 Bangi, Malaysia*
[c] *School of Information, Systems and Modelling, University of Technology Sydney, Ultimo, NSW 2007, Australia*

A B S T R A C T

Aiming at reducing the power consumption and costs of grids, this paper deals with the development of particle swarm optimisation (PSO) based fuzzy logic controller (FLC) for charging–discharging and scheduling of the battery energy storage systems (ESSs) in microgrid (MG) applications. Initially, FLC was developed to control the charging–discharging of the storage system to avoid mathematical calculation of the conventional system. However, to improve the charging–discharging control, the membership function of the FLC is optimised using PSO technique considering the available power, load demand, battery temperature and state of charge (SOC). The scheduling controller is the optimal solution to achieve low-cost uninterrupted reliable power according to the loads. To reduce the grid power demand and consumption costs, an optimal binary PSO is also introduced to schedule the ESS, grid and distributed sources under various load conditions at different times of the day. The obtained results proved that the robustness of the developed PSO based fuzzy control can effectively manage the battery charging–discharging with reducing the significant grid power consumption of 42.26% and the costs of the energy usage by 45.11% which also demonstrates the contribution of the research.

1. Introduction

The rising awareness towards the development of efficient power generation, transmission and distribution issues aims at mitigating the environmental damage caused by the non-renewable energy sources such as coal, petroleum or natural gas. Therefore, the transformation of current electric power systems to renewable sources such as solar power, wind, biomass and tidal power is gaining more popularity as a solution to the power reliability and quality issues (Hossain et al., 2019a; Uzar, 2020; Maleki et al., 2020). Various countries around the world aim to increase power consumption from renewable sources by 20% by 2020. However, this technology requires a storage facility as they are not available throughout the day (Ghasemi and Enayatzare, 2018). Therefore, to expedite the use of renewable sources, the integration of energy storage systems (ESSs) is highly recommended as an effective solution in microgrid (MG) applications (Hossain et al., 2019b).

A MG is a group of interconnected loads and distributed sources, that can be designed in both standalone and grid-connected mode (Haddadian and Noroozian, 2017). A complete architecture of ESS based MG was investigated in Roslan et al.

(2019), as it combines the advantages of AC and DC MGs. The performance of ESSs varies based on the ESS material, charging–discharging capabilities, size, energy density, lifecycle, power electronic interfacing, nature of sources and loads (Faisal et al., 2018). Therefore, the selection of efficient ESSs and their application in MG is still a concern for researchers. Research on energy storage has shown that the trends of ESS application are increasing day by day. Fig. 1 illustrates the development of battery ESS (BESS) technologies with their specific energy density. As shown in the figure, Li-ion storage technology has become widely popular compared to the other storage devices.

In the development of MG systems, controlling the charging–discharging of ESS is necessary, as it can help in supplying power during peak hours and absorbing power during off-peak hours (Hajiaghasi et al., 2019). Various studies have investigated the traditional charging–discharging techniques of the storage. A commonly used CC–CV technique has been used to develop a multi-objective framework for fast-charging protocols considering charging time, ageing and balanced charge (Perez et al., 2017). This analysis proved the importance of temperature and ageing in controlling the battery charging. Other researchers have investigated the applications of pulse charging, reflex charging and trickle charging methods (Zhu and Tatarchuk, 2016; Lai et al., 2017). However, these techniques have the challenges of complexity, over-charging or self-discharging problems, charging

* Corresponding author.
E-mail address: hannan@uniten.edu.my (M.A. Hannan).

Nomenclature

|	
AC	Alternating Current
CC	Common Current
CV	Common Voltage
DC	Direct Current
DG	Distributed Generation
ESS	Energy Storage System
FLC	Fuzy Logic Controller
MF	Membership Function
MG	Microgrid
MPC	Model Predictive Control
PCC	Point of Common Coupling
PSO	Particle Swarm Optimisation
RESs	Renewable Energy Resources
SOC	State of Charge
VPP	Virtual Power Plant
P_d	Power Difference Between DG and Load
$\triangle SOC$	Difference of Reference SOC and Battery SOC
$\triangle T$	Difference of Reference and Battery Temperature
P_{DIE}	Diesel Power
P_{PV}	Photovoltaic Power
P_{WT}	Wind Power
P_{FC}	Power from Fuel Cell
P_{BIO}	Power from Biomass Plant
P_{GRID}	Grid Power
P_{BAT}	Battery Power
P_{DG}	Total Power from Distributed Sources
Q	Battery Capacity
c_1	Social Rate
c_2	Cognitive Rate
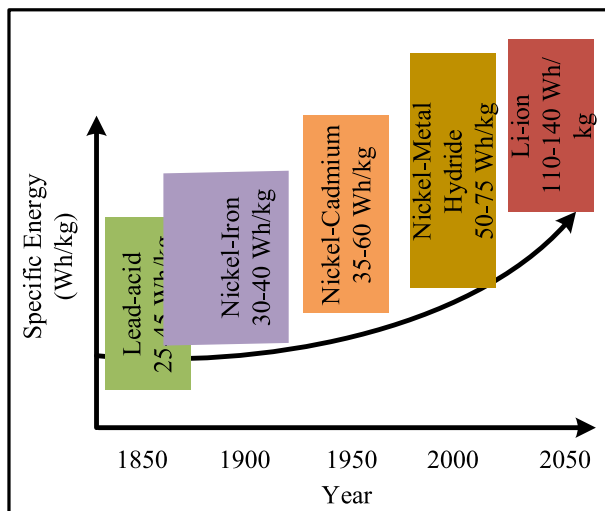
Fig. 1. Development of ESS technology with specific energy density.

period, efficiency and temperature control. The droop control method of ESSs was introduced in Zhu et al. (2018), but this method has the problem of poor harmonic sharing, slow dynamic response and trade-off between voltage regulation and load sharing. To address these issues, model predictive control (MPC) for charging–discharging was investigated in Tang and Wang (2019) and Wang et al. (2019), by which the network

objective function and constraints can be formulated into a finite-time optimal control problem. This technique is suitable for industries, robotics and vehicle navigation (Morstyn et al., 2018). However, MPC does not suitable for nonconvex optimisation problem, and it suffers from complex operation and less flexibility. Authors in Bhowmik et al. (2018) and Mukherjee and De (2017) proposed the proportional–integral controller for controlling the battery charging–discharging, but this controller lacks the ability to realise fast charging–discharging capability. Addressing these challenges of the aforementioned charging–discharging controllers, researchers are now focusing on the powerful fuzzy logic controller (FLC) to model a nonlinear and complex dynamic system that can be implemented to resolve the battery state of charge (SOC) problem. The fuzzy control rule is considered as the knowledge of experienced persons in any field of application, and thus can provide the best decision even in incomplete solution (Mansiri et al., 2018). Moreover, as the membership functions (MFs) are trained offline, it is computationally intensive and can effectively control the battery SOC. The FLC is suitable for uncertain or approximate reasoning; depends on linguistic model; requires no mathematical calculation; and is characterised by smooth controlling, high precision, faster response, and easy implementation (Keshtkar and Arzanpour, 2017). In fact, the input and output MFs of FLC are real variables mapped with linear or nonlinear functions (Keshtkar and Arzanpour, 2017).

In Zhang et al. (2017), FLC-based charging–discharging technique is illustrated to maintain the state-of-health of battery, considering the SOC and power. Fuzzy controlled BESS has been investigated for active power compensation of an MG, where the deviation of SOC is considered when computing the additional power support to the grid (Bhattacharjee and Roy, 2018). To stabilise the power buffer in DC MGs, Takagi-Surgeon fuzzy model is proposed in Vafamand et al. (2019). A fuzzy logic-based maximum power point tracker is proposed in Lalouni et al. (2009), where the authors proved that FLC does not respond to the climatic variation and is thus effective for adjusting the appropriate operating voltage. In recent years, the optimisation technique has been applied aiming to improve the FLC effectiveness. In Leonori et al. (2020), genetic algorithm-based MG energy management system is proposed to improve the energy balance between ESS and grid. Aiming to improve the charging time, life cycle and charging efficiency, optimal charging pattern of lithium-ion batteries using PSO-based fuzzy controller has been demonstrated in Wang and Liu (2015). However, in this research, in conjunction with fuzzy controller, 5-stage constant-current charging is employed for rapid charging. Fuzzy based PSO approach for autonomous green power energy system with hydrogen storage has been studied in Safari et al. (2013). The proposed method reduced the fluctuation in battery SOC towards the increasing of life cycle of the battery. To improve the battery life of sensor nodes, similar method is proposed in Collotta et al. (2017) for industrial wireless sensor networks (IWSNs) scenario. Although temperature has strong impact in the life cycle of the battery, this effect was not considered in these studies. In Li et al. (2020), optimal charging of lithium-ion batteries using PSO was illustrated and compared with the traditional CC–CV. The results showed 3.6% better charging capability after optimisation, which reflected the improvement in increasing the battery lifecycle and efficiency. Moreover, SOC-based fuzzy logic supervisor controlling techniques have been optimised for smart power control in MG (Tidjani et al., 2017). charging–discharging current optimisation for the SOC management of ESSs was investigated in Azzollini et al. (2018). The modified battery model in this research is capable to use in all commercial lead–acid batteries. However, there is still the need for improvement in controlling the SOC of the battery considering temperature (Nithyanandam et al., 2018),

power from the renewable and grid sources and battery SOC at a time. The present research proposed an optimised FLC and has addressed all these parameters to mitigate the challenges of the aforementioned researches. MFs of the FLC have been optimised using particle swarm optimisation (PSO). PSO is chosen as it is robust, can search the very large space of candidate solution with less computational time and requires the adjustment of only few parameters. Moreover, PSO is a proven powerful tool for dealing with global optimisation problems with single- or multi-objective functions (Aghajani and Ghadimi, 2018) containing several local optimal values, and the algorithm quickly converges to the desired pattern.

The balance between the supply and demand with optimal operation of battery storage devices can be adjusted by incorporating the scheduling controller for the optimal operation of the system. In Salcedo-Sanz et al. (2016), a novel coral reefs optimisation algorithm with substrate layer (CRO-SL) is proposed for optimal battery scheduling in MG applications. However, the health function of each coral larva must be computed to evaluate the algorithm effectiveness. Authors in Mallol-Poyato et al. (2016) introduced an adaptive nesting evolutionary algorithm for scheduling of MGs consisting of wind turbines, solar panels and ESS. However, tuning of the parameters of this algorithm is difficult to achieve to obtain the optimal solution. In Abdolrasol et al. (2018), an optimal scheduling controller for a virtual power plant was investigated using binary backtracking search algorithm. As BBSA has 5 steps of operation, hence it is more complex to solve the optimal operation. Computational time also high, which is another limitation of this optimisation algorithm. Artificial bee colony algorithm is proposed for optimal scheduling of hydro-thermal power plants to minimise the cost (Alquthami et al., 2020). The main drawbacks of this algorithm are that it suffers from improper exploitation in solving complicated problems and it requires the new fitness test for new parameter to improve the performance. The optimal power management of grid-connected renewable energy systems has been realised by introducing the droop controller (Chen and Trifkovic, 2018). However, load sharing accuracy is degraded by this technique when the per-unit impedance of each DG is unbalanced, which is the main barrier to apply this technology in the modern power system network. MPC-based smart network of residential building is proposed in Bianchini et al. (2019) to schedule the power exchange and battery charging–discharging considering the thermal comfort, PV power availability, and storage capacity. The aim was to minimise the electricity cost using a two-step optimisation strategy. However, MPC suffers from complex operation and less flexibility. Uncertainties of price and load demand for wind power generation in both grid-connected and islanded modes have been modelled by mixed-integer linear programming model, GA, and day-ahead scheduling (Geramifar et al., 2017; Nemati et al., 2018). In Zolfaghari et al. (2018), adaptive fuzzy gain scheduling is introduced to improve the current and power sharing in parallel-connected PV systems. The fuzzy inference system is optimised using H_∞ theory to reduce the error in the fuzzy system. However, these controlling techniques suffer from limitations such as inadaptability with large load variations, space requirements and inferior quality of model prediction, complex calculation and large computational time. The operational procedures of the scheduling aim to minimise the energy coming from the utility grid, maintaining the charging–discharging of the storage uninterrupted and subsequently reduce the cost of energy consumption. Also, the consumers motivation to buy the energy is primarily cheaper price than utility's price. Hence, reducing the energy consumption from utility grid is the important factor for balancing the cost of consumption with increased use of DGs as the energy sources. Addressing all these issues, aiming to reduce

the costs of power consumption from the grid, this research proposes to implement the binary particle swarm optimisation (BPSO) to schedule the DGs and grid. The cost is minimised through this optimisation, because considering the load demand, BPSO allows the grid only when load demand exceeds the power from battery and DGs. In other cases, the grid remains OFF, thus ensures the optimal use of DGs and battery power towards minimising the cost of power consumption. Like PSO, the BPSO is advantageous as it has less parameters, only two equations to solve the problems, which makes it less complex to obtain the optimal output. Although BPSO has the limitation of premature convergence and low convergence rate, it can be overcome by multiple inertial weight strategy (Too et al., 2019), which is our future scope of study.

Overall, from the literature, the traditional controllers suffer from the rapid temperature rise, uncontrolled overcharging and over-discharging, complex operation and faster charging time. The existing FLC and optimised FLC have overcome most of these issues and increased the life expectancy of the battery. However, considering the temperature constraints and maintaining the safe operating region of battery SOC are still now a great challenge for the researchers. Thus, the obvious contribution of the proposed model is to develop an improved optimised fuzzy model considering the SOC variation, power demand and the temperature to control the battery SOC within the safe operating region. The developed rules in this study successfully controlled the battery charging–discharging which has been optimised to obtain the improved performance. Addition to this, in the present research, in conjunction with the optimised fuzzy-based charging–discharging controller, a scheduling controller using binary PSO (BPSO) is proposed to realise optimal operation of MGs and thus reduce the power demand from the utility grid and energy consumption costs by the proper utilisation of ESS. Here, the grids, ESS and the MGs are scheduled considering the load demand. The results show that the fuzzy-BPSO model effectively reduces the grid power demand and thus reduces the electricity consumption costs from the grid. The proposed method can also be applied to schedule hybrid storage systems which require additional control technique considering the response characteristics and charging–discharging behaviour of the storage devices.

The rest of this paper is organised as follows: First, the proposed architecture of optimal controlling of charging and discharging of battery storage devices is described using a methodological framework. Then, the fuzzy control technique is illustrated in details. Subsequently, the optimisation of MFs of FLC is presented. Then, the scheduling controller is described to minimise the consumption cost. In the following section, the results and analysis with the specific outcomes are presented.

2. MG integrated BESS charging–discharging model

The charging–discharging model developed in this study incorporates distributed sources, loads, a lithium-ion battery storage and a grid, as shown in Fig. 2. The distributed sources include the diesel, PV system, wind turbine, fuel cell (FC) and biomass. However, all the DGs are not available at all the time. Hence, to observe the charging–discharging of the storage, the operating time of each DGs are separated based on availability of the particular sources. So, the total power from all DGs at a particular period is the sum of all available sources for that particular period. As shown in the figure, the load variation for the proposed model is considered within the range of 7 kW to 90 kW, according to the demand at different times of the day. Load 1 to load 9 are varied to get the load variations for specific duration. All the loads have different ratings with different switching time, hence when the breaker of one load is closed, it means the particular
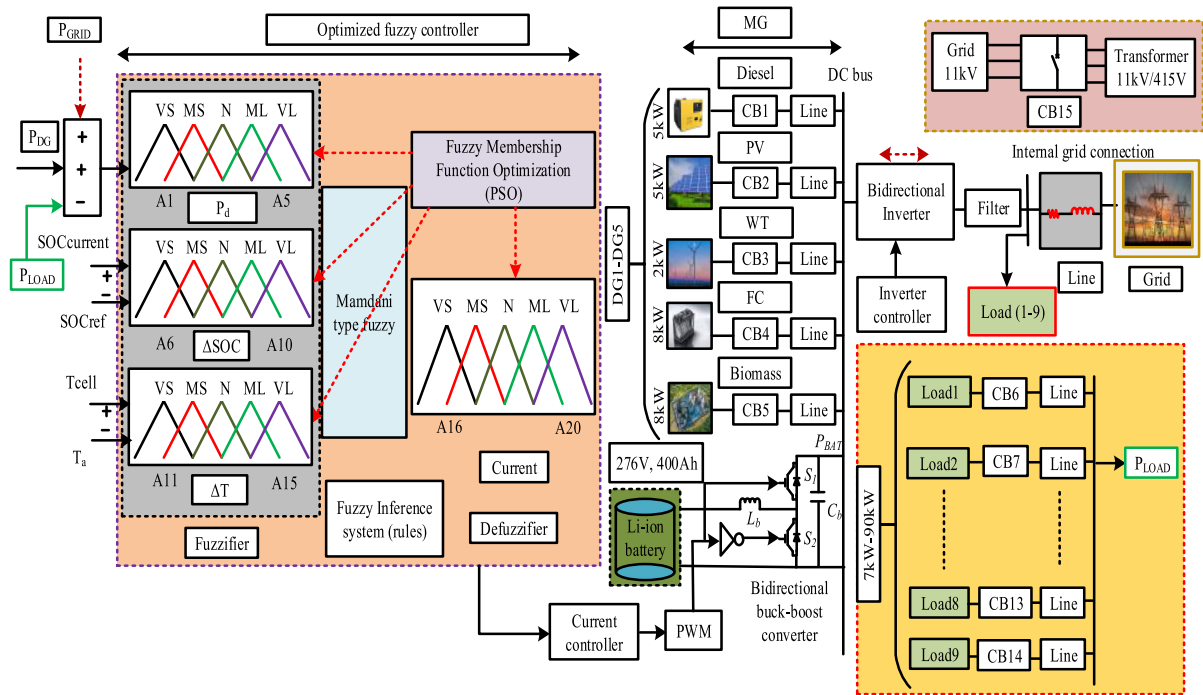
Fig. 2. The proposed fuzzy-based charging–discharging model of lithium-ion battery.

load only is connected with the system at that time whereas the other loads remain disconnected. So, the total load demand for each particular duration is equal to the specific load connected at this time through the circuit breaker. In this research, the lithium-ion battery of 276 V, 400 Ah is chosen as the storage as it has the larger storage capacity, high efficiency, fast charging capability, prolonged lifecycle, and high-energy density (Hannan et al., 2017). Battery integration with the grid is accomplished through bidirectional buck-boost converter, where pulse width modulation technique is used to control the converter. The key role of the converter is to supply the required power to the load from the storage device (Suresh et al., 2020). The battery storage stabilises the dc-link voltage by equalising current at the dc-link capacitor (Bhattacharjee and Roy, 2018). DC bus voltage is 600 V and voltage at PCC is 415 V. The safe SOC region of the battery is selected within 20% and 80%, where, 20% is the minimum and 80% is the maximum threshold of SOC. To evaluate the variation of cell temperature, 25 °C ambient temperature is considered. Transformer voltage rating is 11/0.415kV (Y-Y) and frequency is of 50 Hz. Filter inductance is 0.01 H and filter capacitance is of 0.00001 F. Buck-boost inductance and capacitance are 7.416×10^{-4} H and 1000 μF. The overall charging and discharging are controlled by the FLC considering the available power from the sources (both grid and DG), load demand, state of charge and cell temperature. Thus the inputs of FLC are modelled as P_d (power difference between the available power and load demand), ΔSOC (difference between current battery SOC and reference SOC) and ΔT (difference between battery temperature and ambient temperature). According to the FLC, if the battery SOC reaches to the minimum limit, it does not discharge beyond this threshold and starts to charge again. On the other hand, when the SOC reaches the maximum threshold, then the battery does not accept the charge above this level. The battery can operate in both modes within the minimum and maximum limit. As the FLC output controls the battery charging–discharging, current is therefore the output of the controller. Referring to this figure, fuzzy inference system constitutes the set of the developed rules to control the battery charging and discharging. Each input and

output variable correspond to five fuzzy subsets, denoted as very small (VS), medium small (MS), normal (N), medium large (ML) and very large (VL). Later, the optimisation of fuzzy MFs to improve the battery SOC performance is described.

3. Optimised fuzzy controller for BESS

To illustrate the optimised fuzzy BESS model, the overall architecture can be divided into three categories. Firstly, fuzzy controller is designed to control the charging–discharging of the battery. To design the controller, MFs of the input and output parameters are determined and a set of fuzzy rules have been created to observe the performance of the controller. Performance of the controller depends on the developed rules and the effectiveness of the rules completely depend on the human experience. Hence, the rules should be developed within the boundary conditions of the MFs with the expertise in this field. Secondly, to improve the performance of the controller in controlling the battery charging and discharging, the PSO algorithm is introduced to optimise the fuzzy MFs. Finally, BPSO is performed to schedule the distributed generation (DG), ESS and grid to minimise the cost. The systematic framework of the overall architecture is depicted in Fig. 3.

3.1. Fuzzy controller framework

In this research, the Mamdani-type fuzzy was implemented based on the centre-of-gravity method considering the inputs and output. Regarding the FLC design, all parameters (no. of MFs, mapping, rules) were adjusted by an offline learning process using the MG power, grid power, temperature and battery SOC. It is required as smaller number of linguistic categories can reduce the complexity and subsequently increase the efficiency of the decision-making process during practical implementation. The fuzzy controller gives the rule-based output of current and thus controls the current to the battery. The fuzzy sets occur in their conditions and conclusions, where the conditions are identical to the rule antecedent, and the conclusion is equivalent to the rule consequent.
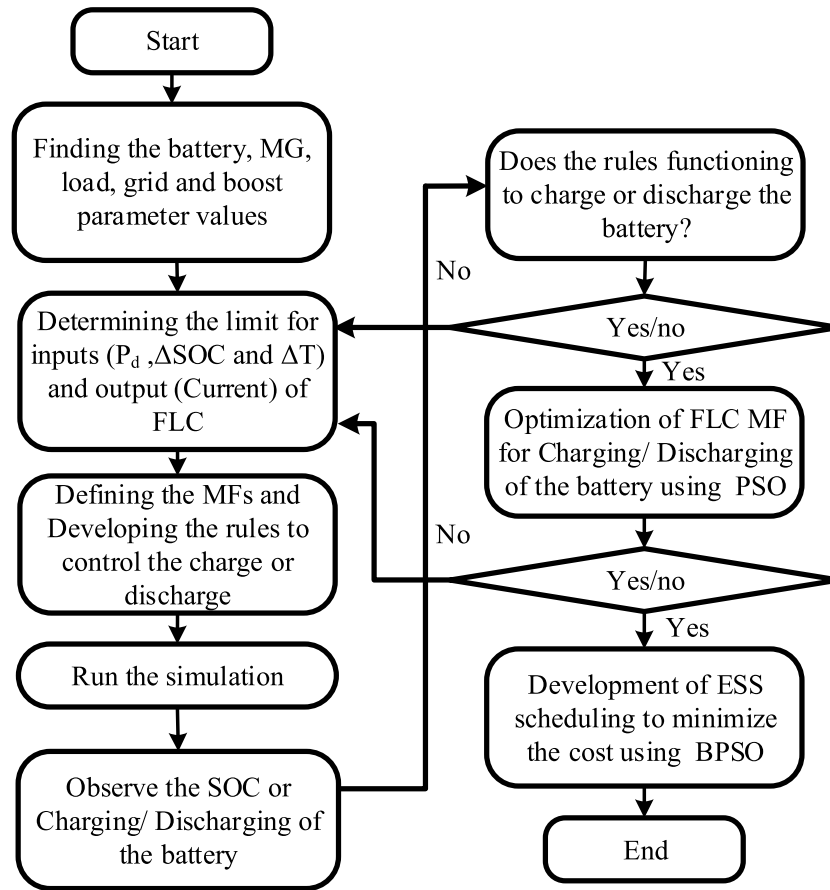
Fig. 3. Systematic framework for optimised BESS.

To determine the P_d, the power from DGs and load demand is calculated according to the following equation:

$$P_d = P_{LOAD} - P_{DG} - P_{GRID} \, (P_{GRID} = 0, \text{ if the grid is OFF}) \tag{1}$$

where P_{LOAD} is the load power and P_{GRID} signifies the surplus grid power after mitigating the load demand. P_{DG} represent the total power from the distributed generations, as shown in Fig. 2. Now, the total distributed power, P_{DG}, can be deduced as,

$$P_{DG} = P_{DIE} + P_{PV} + P_{WT} + P_{FC} + P_{BIO} \tag{2}$$

where P_{DIE}, P_{PV}, P_{WT}, P_{FC}, and P_{BIO} denote power from diesel generator, PV, wind, FC and biomass, respectively.

The total required grid power $P_{GRID,T}$ can be obtained from the total load demand ($P_{LOAD,T}$), total distributed power ($P_{DG,T}$) and the total battery power ($P_{BAT,T}$), as shown from the following equation:

$$P_{GRID,T} = P_{LOAD,T} - P_{DG,T} - P_{BAT,T} \tag{3}$$

Furthermore, $\varDelta SOC$, the other input of FLC, maintains the ranges of the maximum secure limit (SOC_{MAX}) and minimum secure limit (SOC_{MIN}) to preserve the battery lifetime and efficiently control the charging–discharging. When the SOC reaches at 20%, whatever the demand is, the battery will get charged. When the SOC is greater than 80%, the battery can discharge or no action would be taken, according to the demand.

The SOC estimation can be measured by the condition:

$$SOC_{MIN} \leq SOC_{(n)} \leq SOC_{MAX}$$

In this study, the battery SOC limit is chosen to vary from 20% to 80%. Therefore, $\varDelta SOC$ can be calculated by the following equation:

$$\varDelta SOC = SOC_{current} - SOC_{ref} \tag{4}$$

Considering I as the battery current, and Q as the nominal battery capacity, the general equation to evaluate the battery SOC can be written as,

$$SOC = 100 \left(1 - \frac{\int_0^t I dt}{Q} \right) \tag{5}$$

Accordingly, $\varDelta T$ is controlled not to exceed the minimum and maximum limits to protect the battery from damage. Considering the 25 °C ambient temperature, the range of $\varDelta T$ is limited within 0° to 35 °C as the safe operating region. Here, the ambient temperature is kept constant as different operating temperature affects the performance of battery over time at different rates and subsequently reduces the life time. For rapid evaluation of the cell temperature, the equivalent electric thermal model of the lithium-ion battery is illustrated in Motapon et al. (2017). According to this model, the battery temperature (T_{cell}) can be evaluated from the following equation:

$$T_{cell}(t) = L^{-1} \left(\frac{1}{1 + s \cdot t_c} \cdot (R_{th} \cdot P_{loss}(s) + T_a(s)) \right) \tag{6}$$

where $T_a(s)$ is the Laplace transform of ambient temperature (°C), R_{th} is the thermal resistance of the battery equivalent circuit, t_c is the thermal time constant and $P_{loss}(s)$ is the Laplace transform of power loss. The power loss during discharge and charging process includes the polarisation loss, internal resistance loss, and losses due to electrochemical reaction. In this research, during matlab simulation, the cell temperature was observed directly

Table 1
Fuzzy rules.

I		P_d				
		VS	MS	N	ML	VL
$\Delta SOC, \Delta T$	VS/VS	VS	VS	VS	VS	VS
	MS/MS	VS	VS	N	ML	ML
	N/N	VS	MS	N	ML	ML
	ML/ML	VS	MS	N	ML	VL
	VL/VL	N	N	N	ML	VL

VS = Very small, MS = Medium small, N-Normal, ML-Medium large, VL = Very large.

by activating the temperature affect in the lithium-ion battery model.

Now, as shown in the proposed model, the other input of FLC, the temperature difference (ΔT) between cell (T_{cell}) and ambient temperature (T_a) can be evaluated by

$$\Delta T = T_{cell} - T_a \tag{7}$$

Throughout the system implementation, boundaries and the step leaders (A0, A1… A20, as shown in Fig. 2) are arranged such that no one can overlap the other. Conditions of not overlapping can be deduced as

$$A(t-1) < A(t) < A(t+1), \text{ where } t = 0, 1, 2, \ldots, 20. \tag{8}$$

Thus, constraints for fuzzy charging–discharging optimisation can be expressed as

$$\begin{aligned} \Delta SOC_{MIN} &\leq \Delta SOC_{(n)} \leq \Delta SOC_{MAX} \\ P_{d,MIN} &\leq P_{d(n)} \leq P_{d,MAX} \\ \Delta T_{MIN} &\leq \Delta T_{(n)} \leq \Delta T_{MAX} \end{aligned} \tag{9}$$

These constraints control the fuzzy output current to battery for efficient charging–discharging.

As shown in Table 1, 25 rules have been designed to regulate the battery charging–discharging. First rule of the table shows that, if ΔSOC is VS, ΔT is VS, P_d is VS, then the output current I is VS. This rule illustrates that if the battery SOC and temperature are low and the demand is high enough, the battery operates in charging mode. Following this, rule 25 of the table reveals that if ΔSOC is VL, ΔT is VL, P_d is VL, then the output current I is VS. It implies that if the battery SOC is high, temperature also becomes high, and therefore, with a low load demand, the battery operates in discharging mode.

Overall, if the SOC goes below the acceptable range, the battery surely charges irrespective of the load demand. On the other hand, if the battery SOC peaks at its maximum limit, then it does not accept the charge, thus protecting the battery from over-charging or over-discharging.

3.2. Fuzzy-based PSO for charging–discharging

In general, fuzzy sets cannot distinguish the differences between the positive and negative information of MFs. However, a balanced fuzzy set theory is essential to develop an optimal algorithm. Accordingly, in this research, fuzzy-based PSO solves the optimisation problems on the boundary information of the MF of power difference, SOC and temperature difference of the battery.

PSO is a computational method to iteratively find the optimal solution by improving a candidate solution based on the given measure of quality (Hossain et al., 2019a). It solves the problem using the population of particles and by moving these particles in the search space following simple mathematical formulae over the particle's position and velocity. According to this theory, each

Table 2
Framework of PSO for battery charging–discharging.

Input: $Problem_{Size}$, $Population_{Size}$
Output: P_{gBest}
$Population \leftarrow \varphi$, $P_{gBest} \leftarrow \varphi$
For $N = 1$ to $Population\ Size$ **do**
$P_{Velocity} \leftarrow$ Random Velocity(), $P_{Position} \leftarrow$ Random Position($Population_{Size}$)
$P_{pBest} \leftarrow P_{Position}$
if ($SOC(P_{pBest}) \leq SOC(P_{gBest})$)
$P_{gBest} \leftarrow P_{pBest}$
end; end
while ($i \leq iteration_{max}$)
for($P \in Population$)%Update velocity
$P_{Velocity} \leftarrow$ Update velocity ($P_{Velocity}, P_{gBest}, P_{pBest}$)
$P_{Position} \leftarrow$ Update position ($P_{Position}, P_{Velocity}$)
if ($SOC(P_{Position}) \leq SOC(P_{pBest})$)
$P_{pBest} \leftarrow P_{Position}$
if ($SOC(P_{pBest}) \leq SOC(P_{gBest})$)
$P_{gBest} \leftarrow P_{pBest}$
end; end; end; end
return (P_{gBest})

particle swarm reflects a solution in the solution space, and each particle i has a current position, current velocity and personal best position in the search space, denoted by X_i^d, V_i^d and P_i^d, respectively. The particle first searches the local best position for each iteration, and then the global best position is determined from all previous iterations. Equations for PSO to determine the updated position and velocity can be expressed as,

$$\begin{aligned} V_i^d(t+1) = {}& wV_i^d(t) + c_1 r_1 \left(P_i^d(t) - X_i^d(t) \right) \\ & + c_2 r_2 \left(P_t^d(t) - X_i^d(t) \right) \end{aligned} \tag{10}$$

$$X_i^d(t+1) = X_i^d(t) + V_i^d(t+1) \tag{11}$$

Here, $V_i^d(t+1)$ and V_i^d respectively denote the update and current velocity of the particles, while $X_i^d(t+1)$ and X_i^d respectively represent the update and current position; w is the inertia weight; c_1 and c_2 are the social rate and cognitive rate, respectively; and r_1 and r_2 are random values within the interval (0, 1). It is noted that PSO has the limitation to get the optimal solution when the algorithm falls around the local minimum. To solve this issue, the appropriate inertia weight w can be chosen, the parameters r_1 and r_2 can be adjusted to obtain the better solution and make the convergence speed faster (Gao et al., 2019). Table 2 presents the steps of the PSO algorithm.

According to this algorithm, first, the PSO parameters are initialised with the swarm size, problem dimension and iteration number. Following this initialisation step, the objective function is estimated for each particle, and the velocity and position are updated. Therefore, personal best (*pbest*) and global best (*gbest*) are determined. Personal and global positions lead the particle towards a suitable direction and augment the prospect to find the global best solution. The updated velocity and position are used to evaluate the objective function again. Therefore, to accelerate the convergence, the inertia weight factor w decreases with the increasing iteration.

$$w = \frac{w_{max} - w_{min}}{iteration_{max}} \times iteration \tag{12}$$

where w_{max} and w_{min} are the maximum and minimum inertia weights, respectively; *iteration* is the current iteration number and $iteration_{max}$ is the maximum allowable iteration. Moreover, as the defuzzification generates the suitable crisp value from the FLC, the best boundaries of MFs need to be determined. As the output parameter of the FLC is current, and the rules have been created to control the current, hence, to ensure the smooth operation and to control the overcharging or over-discharging of
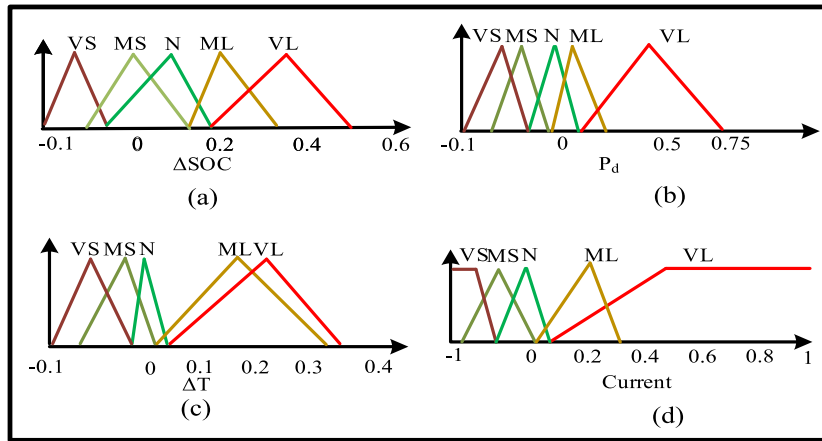
Fig. 4. Optimised MF using PSO: optimised MFs for (a) ΔSOC; (b) P_d;(c) ΔT; (d) current.

the battery, the objective function can be expressed as,

$$Objective\ function = \min\left[\sum_{i=1}^{N} I(t_i)\right] \tag{13}$$

where, $I(t_i)$ denotes the battery current (to/from) for charging/discharging at time t_i. Hence, following the mean square error (MSE) technique, considering the estimated value (I_{est}) and actual value (I_{actual}), the function $I(t_i) = (I_{est} - I_{actual})^2/N$ determines the optimal solution by obtaining the minimum value of the objective function through iteration. When charge drawn/supplied by the battery, the estimated value of the battery current can be monitored by using Eq. (5). To obtain the fuzzy output, in this research, centre of gravity is used, and the expression for obtaining the output is as follows:

$$Output_{crisp} = \frac{\sum_{i}^{n} w_i I_i}{\sum_{i}^{n} w_i} \tag{14}$$

where $output_{crisp}$ denotes the controller output, I is the output value of MFs and n is the rule number. Now, in addition to Eqs. (8) and (9), the additional constraints for charging–discharging can be formulated as

$$\sum_{t=1}^{T} (P_{DIE}(t) + P_{PV}(t) + P_{WT}(t) + P_{FC}(t) + P_{BIO}(t) + P_{GRID}(t))$$

$$> \sum_{t=1}^{T} P_{LOAD}(t) \quad \text{(for charging)} \tag{15}$$

$$\sum_{t=1}^{T} (P_{DIE}(t) + P_{PV}(t) + P_{WT}(t) + P_{FC}(t) + P_{BIO}(t) + P_{GRID}(t))$$

$$< \sum_{t=1}^{T} P_{LOAD}(t) \quad \text{(for discharging)} \tag{16}$$

Eq. (15) depicts that, for charging, there must have the surplus generated power compare to the load demand, whereas, Eq. (16) shows that, the battery discharges if the generated power becomes less than the load demand. The output of the proposed charging–discharging model is optimised by optimising the input and output MFs of the FLC. Optimised fuzzy MFs for each input and output are shown in Fig. 4. 100 iterations are used to optimise the fuzzy output. It shows that, the objective function reaches its minimum value after 93 iterations, which is depicted in Fig. 5.
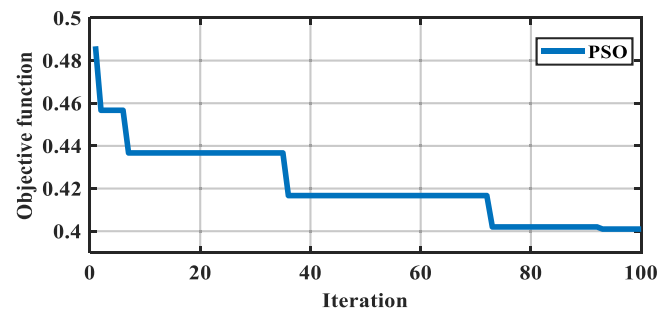

Fig. 5. Objective function of PSO.

3.3. Fuzzy-based PSO for scheduling controller

A scheduling controller is adopted to schedule ON and OFF of the distributed sources, battery storage and grid according to the load demand aiming to minimise the consumption cost. Therefore, suitable source can be selected for economically optimal dispatch through this controller. Since the distributed sources such as solar and wind mostly depend on several factors, such as weather condition and temperature, the power from these sources are not always available. Fig. 6(a) shows the wind speed, and Fig. 6(b) depicts the solar irradiance at different times of a particular day. The solar irradiance is shown to be maximum at noon, and from 7:30 PM to 6 AM, it is almost zero, and therefore, no solar power can be produced at this time.

Consequently, an optimised algorithm is mandatory to manage the energy demand for the loads. Therefore, fuzzy-based BPSO is proposed to solve the optimisation problem on the operational constraints of the available sources and loads to minimise the objective function of mean cost by reducing the grid energy consumption. Constraints to manage the optimisation can be formulated as follows:

Production capacity:

Each power unit of the DG should produce energy within the capacity:

$$P_{DG,\min}(t) \leq P_{DG}(t) \leq P_{DG,\max}(t)$$

$$P_{GRID,\min}(t) \leq P_{GRID}(t) \leq P_{GRID,\max}(t) \tag{17}$$

$$P_{BAT,\min}(t) \leq P_{BAT}(t) \leq P_{BAT,\max}(t)$$
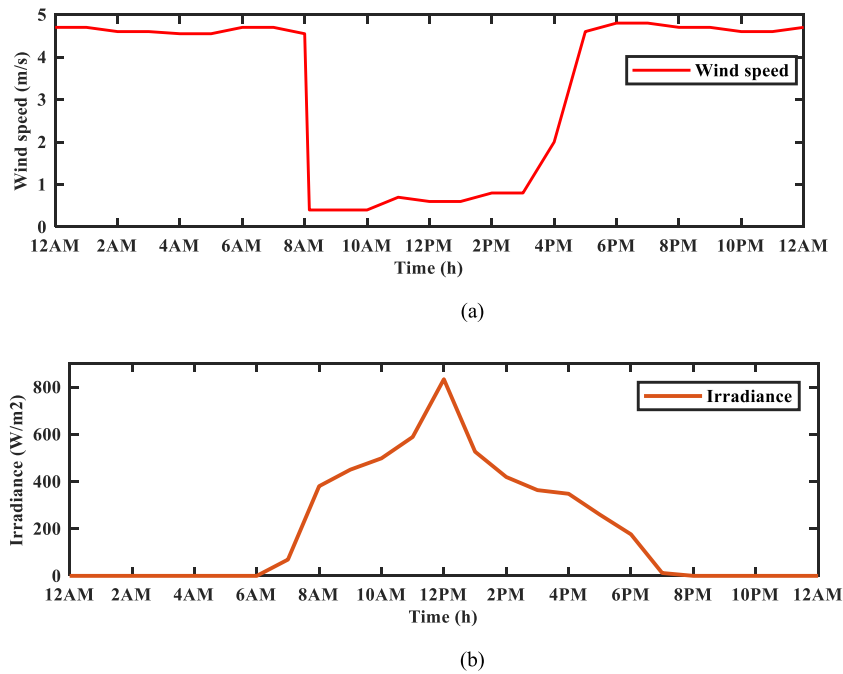
Generation and load balance:

Fig. 6. Solar irradiance and wind speed data: (a) wind speed (m/s); (b) solar irradiance (W/m²).

The total amount of power produced by DGs, grids and power should manage the load demand.

$$\sum_{t=1}^{T} (P_{DIE}(t) + P_{PV}(t) + P_{WT}(t) + P_{FC}(t) + P_{BIO}(t) + P_{BAT}(t))$$

$$= \sum_{t=1}^{T} (P_{LOAD}(t) - P_{GRID}(t)) \tag{18}$$

Load and battery charging–discharging limitation:

The load demand cannot be more than the total generated power from battery, grid and DGs. Therefore, charging and discharging of the battery should not cross the minimum and maximum charging or discharging capacities.

$$P_{Ch\,arg\,e}(t) \leq P_{Ch\,arg\,e,\max}(t) \tag{19}$$

$$P_{disch\,arg\,e}(t) \leq P_{disch\,arg\,e,\max}(t)$$

As the objective function is to minimise the cost and reduce the grid energy consumption, uncertainties considered for the power from the diesel, PV, WT, grid energy cost and load can be modelled as

$$P_{DIE}(t) = P_{DIE}^{forecast} + \Delta P_{DIE}$$

$$P_{WT}(t) = P_{WT}^{forecast} + \Delta P_{WT}$$

$$P_{PV}(t) = P_{PV}^{forecast} + \Delta P_{PV} \tag{20}$$

$$P_{LOAD}(t) = P_{LOAD}^{forecast} + \Delta P_{LOAD}$$

$$Pr\,ice_{GRID}(t) = Pr\,ice_{GRID}^{forecast} + \Delta Price_{GRID}$$

where ΔP_{DIE}, ΔP_{WT}, ΔP_{PV}, ΔP_{LOAD}, $\Delta Price_{GRID}$ are the forecasted diesel power output error, wind power output error, solar power output error, forecasted load power error and forecasted market price error.

The proposed method involves finding the best schedule to regulate the power dispatch from the sources, and thus, the cost is minimised. In this research, BPSO is used as the scheduling controller as it requires less computational time and is easy to implement. Twenty swarms were selected for this purpose, where each swarm represents a cell (schedule). The iteration ran for 100
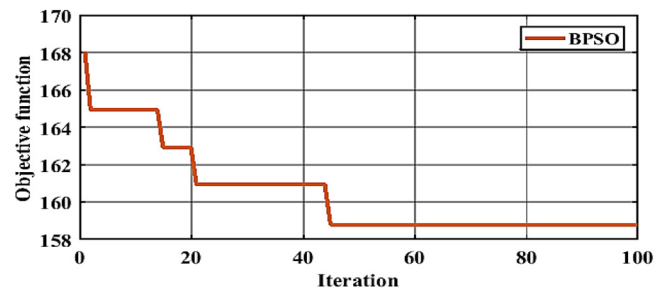

Fig. 7. Objective function of BPSO.

loops. The output of the objective function after completing the operation is shown in Fig. 7.

The obtained plot shows that the minimum cost was attained after 45 iterations. The particles in BPSO are represented as a bit string or binary, the value of which may be either 0 (OFF) or 1 (ON). To perform this task, initially a matrix of 7 columns and 24 rows was formed. Equations for generating random schedule in decimal and then converting to binary can be expressed as

$$swarm_{(h,s)} = rand \cdot \begin{bmatrix} swarm_{(1,1)} & \cdots & swarm_{(1,s)} \\ \vdots & \ddots & \vdots \\ swarm_{(h,1)} & \cdots & swarm_{(h,s)} \end{bmatrix} \tag{21}$$

$$swarmB_{(h,s)} = rand \cdot \begin{bmatrix} swarmB_{(1,1)} & \cdots & swarmB_{(1,s)} \\ \vdots & \ddots & \vdots \\ swarmB_{(h,1)} & \cdots & swarmB_{(h,s)} \end{bmatrix} \tag{22}$$

where *swarm* and *swarmB* define the random decimal population matrix and random binary population matrix, respectively. Moreover, $h = 1, 2, 3 \cdots \cdots, 24$ denotes the hours in a day and $s = 1, 2, 3 \cdots \cdots, 7$ is the status of DG, grid and battery switches. The best cell is stored in P_{best_TD} and P_{best_TB}, for decimal and binary population matrix, respectively. Equations for the total can

be expressed as

$$swarmT_{(1,k)} = \left\{ \begin{bmatrix} swarm_{(1,1)} & \cdots & swarm_{(1,s)} \\ \vdots & \ddots & \vdots \\ swarm_{(h,1)} & \cdots & swarm_{(h,s)} \end{bmatrix} \cdots \right.$$
$$\left. \times \begin{bmatrix} swarm_{(1,1)} & \cdots & swarm_{(1,s)} \\ \vdots & \ddots & \vdots \\ swarm_{(h,1)} & \cdots & swarm_{(h,s)} \end{bmatrix}_{(1,k)} \right\} \quad (23)$$

$$swarmTB_{(1,k)} = \left\{ \begin{bmatrix} swarmB_{(1,1)} & \cdots & swarmB_{(1,s)} \\ \vdots & \ddots & \vdots \\ swarmB_{(h,1)} & \cdots & swarmB_{(h,s)} \end{bmatrix} \cdots \right.$$
$$\left. \times \begin{bmatrix} swarmB_{(1,1)} & \cdots & swarmB_{(1,s)} \\ \vdots & \ddots & \vdots \\ swarmB_{(h,1)} & \cdots & swarmB_{(h,s)} \end{bmatrix}_{(1,k)} \right\}$$
$$(24)$$

where k is population size, and $swarmT$ and $swarmTB$ are the totals of all $swarm$ and $swarmB$ cells, respectively.

Following this step, the conversion from decimal to binary using sigmoid function can be deduced as

$$sigmoid\left(T_{\{i\}}\right) = \frac{1}{1 + e^{-T_{\{i\}}}} \quad (25)$$

$If\ sigmoid > rand \quad then\ TB_{\{i\}} = 1 \quad else\ TB_{\{i\}} = 0$

The minimum evaluation and $swarm\_TD\{best\}$ is stored at f_{best} and g_{best}, the location of minimum evaluation is $best$; therefore,

$$[f_{best}, best] = \min(Evaluation) \quad (26)$$

$$g_{best} = swarm\_TD\{best\} \quad (27)$$

Following equations (7) and (8), the update velocity and position can be written as

$$v\{k+1\} = w \times v\{k\} + c_1 \times rand \times (P_{best}\_TD\{k\}$$
$$- swarm\_TD\{k\}) + c_2 \times rand \times (g_{best} - swarm\_TD\{k\}) \quad (28)$$

$$new position = swarmTD\{k\} + v\{k+1\} \quad (29)$$

$$swarm\_TD\{k\} = new\_position \quad (30)$$

The objective function is to minimise the cost, and can be expressed as,

$$Objective\ function = \min\left[\sum_{t=1}^{T} P(t)\,(cost\,t/kWh)\right] \quad (31)$$

$$P(t) = \frac{3}{2}IV \times power\ factor \quad (32)$$

where $P(t)$ denotes the power consumption from the grid, I is the current, V is the voltage, T is the time, and cost/kWh indicates the per unit cost of electricity in an hour. Thus, the best schedule to minimise the cost can be obtained from the minimum evaluation and best cell P_{best}_TB. Therefore, cost saving depends on both the DG and battery. For a fixed battery, costs savings increases with larger DGs as the payback time of the overall system decreases, and for the fixed DGs, costs savings grows as the battery size increases, and if the battery size crosses the threshold limit, the system payback time increases. In this research, only the operation cost is considered. Therefore, for the Malaysian perspective, total cost/day is calculated using the following equation:

$Cost(RM/Day)$
$$= \frac{Energy\ consumption\ in\ kWh\ per\ day \times Cost(cent/kWh)}{100}$$
$$(33)$$

Table 3
Analysis of battery charging–discharging behaviour.

Time	Grid	DG	Condition	Battery
0–0.1 s	OFF	ON	$P_{LOAD} > P_{DG}$	Discharging
0.1–0.2 s	OFF	ON	$P_{DG} > P_{LOAD}$	Charging
0.2–0.4 s	OFF	ON	$P_{LOAD} > P_{DG}$	Discharging
0.4–0.5 s	OFF	ON	$P_{LOAD} > P_{DG}$	Discharging
0.5–0.8 s	ON	ON	$P_{GRID} > P_{LOAD}$	Charging
0.8–0.9 s	OFF	ON	$P_{DG} > P_{LOAD}$	Charging
0.9–1 s	OFF	ON	$P_{DG} > P_{LOAD}$	Charging

4. Results and discussions

To illustrate the performance of the developed model for battery charging–discharging, firstly, load demand of the consumers and power from DG, along with their differences, are depicted in Fig. 8. The figure shows that the load varied according to the consumer demand at different periods. For simulation purpose, to prove the robustness of the proposed controller under rapid fluctuation of the load, we have shown the various load variation within 1 s, whereas, the minimum and maximum load are 7 kW and 90 kW, during 0.1–0.2 s and 0.4–0.5 s, respectively. The output of FLC, i.e., current, was controlled based on the developed rules to supply the power to the load. The FLC is designed to charge the battery when the power is available and discharges when the demand exceeds the generated power. Later, PSO was introduced to improve the controlling performance of the battery SOC.

Fig. 9 shows the temperature effect when controlling the battery charging–discharging. From the figure, it is clear that, without fuzzy, the cell temperature rose rapidly from the initial level of 25 °C to 38 °C after 1 s, while, with fuzzy, the initial rapid peak was reduced, and it continued throughout the operation. Thus, following the conditions during the development of fuzzy controller, the temperature rise dropped at about 34 °C within the same period. Fuzzy PSO reduced the battery temperature more and reached 33 °C at this time. Therefore, considering the ambient temperature, fuzzy PSO showed better performance compared with the fuzzy-only system.

Moreover, the results show that the battery SOC was controlled by both the charging and discharging. Figs. 10 and 11 reflect the SOC and current output for both fuzzy and fuzzy PSO conditions. As the grid is initially OFF, and the load demand is greater than the distributed generation (Fig. 8), hence, the battery discharges through the load. From Fig. 10, the battery SOC shows decreasing trend within 0–0.1 s and the discharging battery current also reveals in Fig. 11. From 0.1–0.2 s, the distributed generation exceeds the load demand (Fig. 8), hence the battery SOC is increasing (Fig. 10) and the battery current also shows the charging trend (Fig. 11). The other charging or discharging cases also can be explained in the similar way except the time duration 0.5–0.8 s, where, the grid is ON, and meets the load demand. Hence, the battery charges within this period as the total generated power from grid and DG becomes greater than the load demand. The overall performance of fuzzy and fuzzy PSO output with respect to the load demand, grid operation, DG power and ESS condition is tabulated in Table 3.

According to the table, the grid operated from 0.5–0.8 s only, while battery was charging or discharging, based on the load demand. From 0–0.1 s and 0.2–0.5 s, the battery discharged, while for the other cases, the battery charged. Overall, from the analysis of Figs. 10 and 11, it is observed that the battery SOC control was improved by the optimised fuzzy system than the fuzzy-only system, and moreover, the battery current was more stable in the optimised fuzzy. Therefore, the objective to improve the SOC control with the optimised PSO was achieved. Overall,
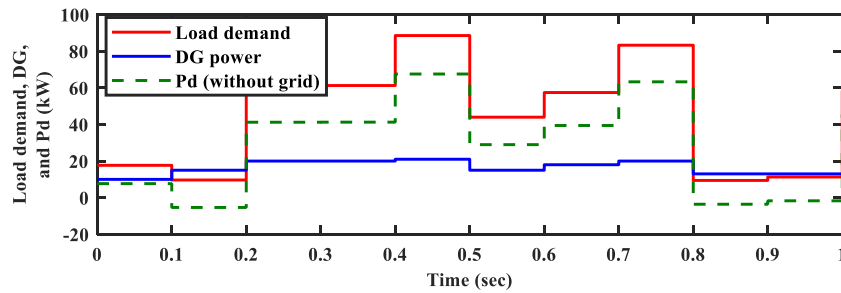
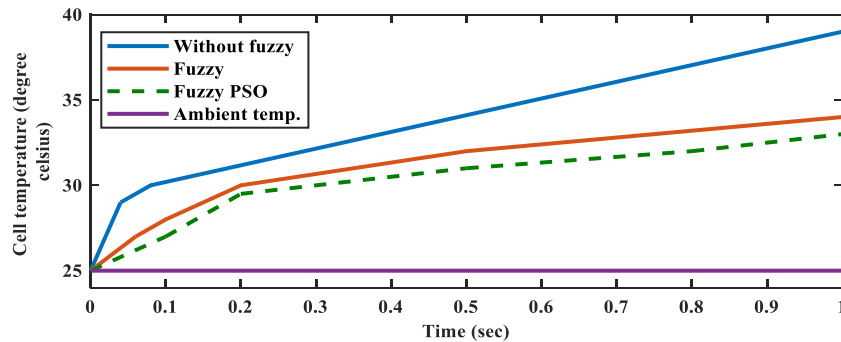**Fig. 8.** DG power, load demand and their differences.

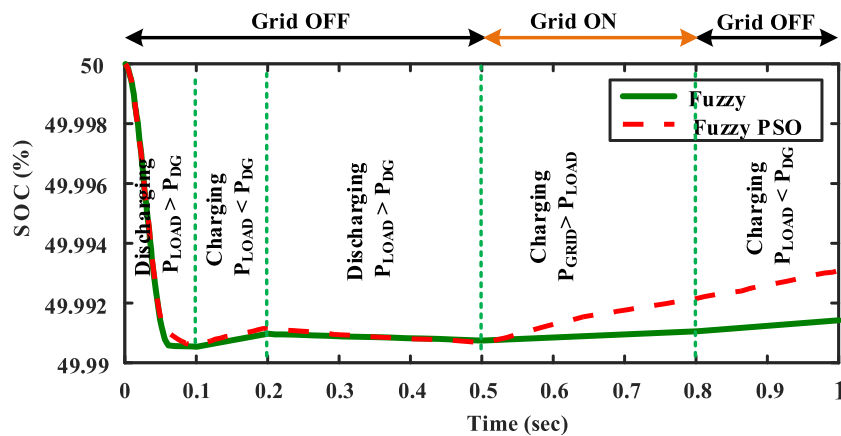**Fig. 9.** Cell temperature curve without fuzzy, with fuzzy and with optimised fuzzy.

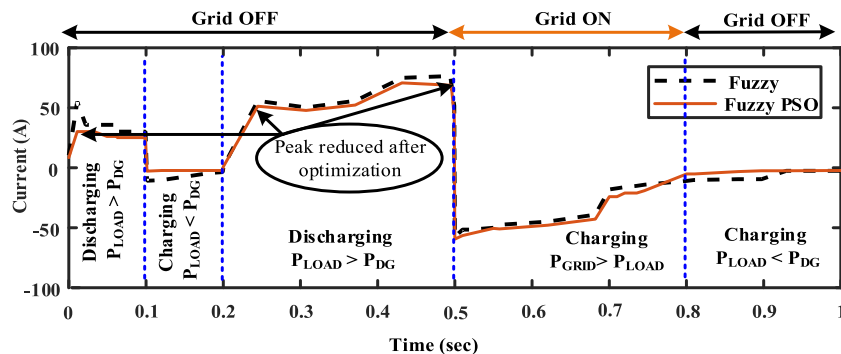**Fig. 10.** SOC with fuzzy and optimised fuzzy.

Fig. 11. Battery current with fuzzy and optimised fuzzy.

it can be said that the contribution of this research is proven to control the battery charging–discharging of the battery under sudden load variation towards increasing the life expectancy of

the battery. It is also seen that, within this short duration, the optimised FLC outperforms the fuzzy only system in faster battery charging (0.5–1 s, as shown in Fig. 10), which in turns proves
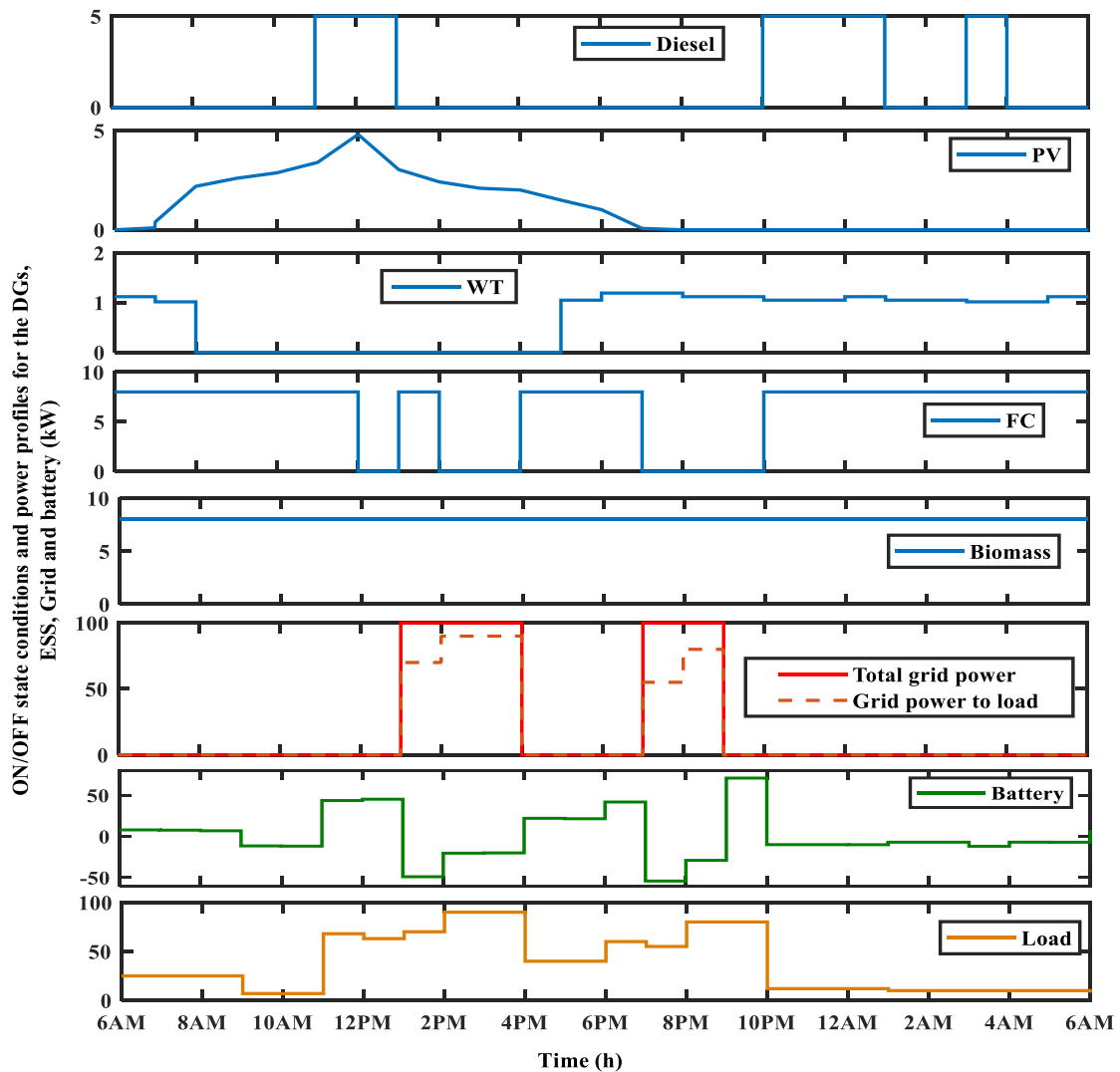
(a)
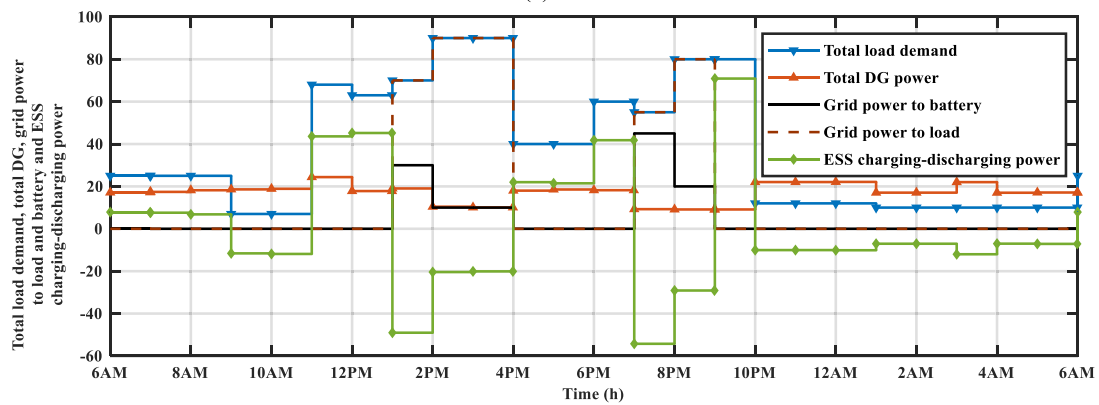
(b)

Fig. 12. (a) Individual DG power, grid power, battery power and load curve (b) Aggregated DG power and grid power profile to the load for charging–discharging of the battery.

the robustness of the proposed optimised topology compare to unoptimised fuzzy only system for long time operation of battery charging–discharging. Similar research on fuzzy PSO system with hydrogen storage (Safari et al., 2013), showed the load variation

after every 1 h, which does not prove the robustness in response to sudden load variation. Another significant limitation of this research is not considering the temperature, which is the significant parameter of the battery. Another research on similar control

Table 4
BPSO scheduling controller operation.

Input data	BPSO Scheduling Algorithm									Battery status
	Energy Management System (EMS)									
	Hour	Diesel	PV	WT	FC	Biomass	Grid	BESS	Load	
Grid data	6 AM	0	0	1	1	1	0	1	25	Discharging
	7 AM	0	1	1	1	1	0	1	25	Discharging
	8 AM	0	1	0	1	1	0	1	25	Discharging
	9 AM	0	1	0	1	1	0	0	7	Charging
	10 AM	0	1	0	1	1	0	0	7	Charging
	11 AM	1	1	0	1	1	0	1	68	Discharging
	12 PM	1	1	0	0	1	0	1	63	Discharging
	1 PM	0	1	0	1	1	1	0	70	Charging
	2 PM	0	1	0	0	1	1	0	90	Charging
Weather Data	3 PM	0	1	0	0	1	1	0	90	Charging
	4 PM	0	1	0	1	1	0	1	40	Discharging
	5 PM	0	1	0	1	1	0	1	40	Discharging
	6 PM	0	1	1	1	1	0	1	60	Discharging
	7 PM	0	1	1	0	1	1	0	55	Charging
Load	8 PM	0	0	1	0	1	1	0	80	Charging
	9 PM	0	0	1	0	1	0	1	80	Discharging
	10 PM	1	0	1	1	1	0	0	12	Charging
	11 PM	1	0	1	1	1	0	0	12	Charging
	12 AM	1	0	1	1	1	0	0	12	Charging
	1 AM	0	0	1	1	1	0	0	10	Charging
	2 AM	0	0	1	1	1	0	0	10	Charging
	3 AM	1	0	1	1	1	0	0	10	Charging
	4 AM	0	0	1	1	1	0	0	10	Charging
Battery	5 AM	0	0	1	1	1	0	0	10	Charging

technique reveals that, the battery charges when the battery SOC goes below the lower threshold 50% and the load variation also was between 100 kW to 110 kW throughout the simulation (Zhao et al., 2015). Here also temperature was avoided. Hence, it is proven that the proposed optimised topology shows the robustness in wide variation of load within shortest duration.

The BPSO algorithm generates a binary schedule of 1 or 0, for ON and OFF states, respectively. The BPSO schedules the distributed sources, grid and battery storage devices for mitigating the load demand and thus saves energy and consumption cost. Table 4 presents the best schedule to manage the energy crisis based on the load demand. Fig. 12 is the graphical representation of the energy management behaviour for the proposed scheduling controller. Fig. 12(a) illustrates the power profile during the ON and OFF states of the individual distributed sources, grid and battery based on the load demand. It shows that the distributed sources, grid and battery supplied the power to the load according to the load demand in 24 h duration. Here, the grid power is assumed to be uninterrupted during the time of operation. As the solar irradiance is high between 7AM to 7PM, hence the PV generates power as shown in Fig. 12, and it reaches peak at 12PM. The wind power generation also shows the real data at any particular day in Malaysia based on the real wind speed at that day. The grid power profile shows that, it remains ON to meet the load demand between 1PM–4PM and 7PM–9PM. Fig. 12(b) shows the accumulated output of the distributed sources, thus shows the clear architecture of the power balance of the battery and grid with respect to load demand. This figure clearly demonstrates that, the surplus generated power after mitigating the load demand goes to charge the battery, in both grid ON and OFF mode. When the grid is OFF, if the total distributed power becomes greater than the load demand, the surplus amount is used to charge the battery. On the other hand, when the total distributed power becomes less than the load demand, the battery supplies power to the load. The supplied and absorbed battery power is depicted in Fig. 12. It is also seen that, when the grid is ON, the total load demand is mitigated by the grid power, hence the surplus amount of total power is used to charge the battery.
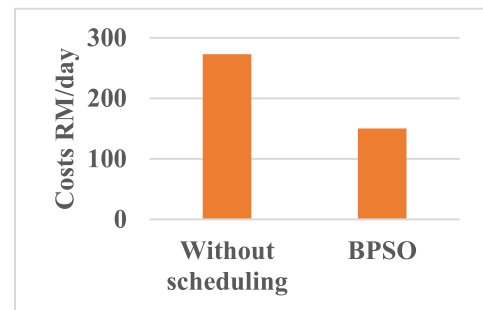

Fig. 13. Cost without scheduling and with scheduling.

Throughout the day, when the grid is ON, the battery does not supply the power to the load. However, when the load demand is less than the total distributed power, then only the DG mitigates the load demand. For other cases, both DG and battery work together to supply the power to the load. The benefit of this scheduling is directly related to the less energy consumption from the grid; thus the scheduling reduces the consumption cost, which is the main objective of developing this controller (Yamchi et al., 2019). The total energy required from the utility grid to mitigate the load demand is calculated as 911 kWh. When the optimal MG scheduling with the renewable energy sources and ESSs were adopted, the total grid power consumption by the load reduced to 385 kWh which is 42.26% of the total load demand. According to the Malaysian tariff rate, the per-kWh cost of electricity consumption varies from 21.8 to 57.10 cent/kWh in the domestic sector. Therefore, considering the average cost/kWh as 30 cents, the total cost without scheduling and in full grid-connected mode reaches 273.3 RM /day. However, as shown in Fig. 13, with scheduling and battery storage system, the result shows that the minimum cost with this scheduling was RM 150/day. Therefore, the total amount of the cost saved was RM 123.3/day (45.11%).

5. Conclusion

This paper presents the FLC to control the charging–discharging of a li-ion battery and achieves an optimal SOC through MF optimisation by the PSO algorithm. The simulation results show that the performance of the battery SOC control was improved, and thus, the current supply to the load was limited. The objective of this study is validated through the scheduling controller, which minimises the consumption cost. In addition, to make the overall system cost-effective, with the developed FLC for the efficient charging–discharging of ESS, an optimal scheduling controller is proposed which provided the best schedule of supplying power from the grid, battery and distributed sources to the loads. This technique proves the efficiency and economic feasibility of the controller by reducing the significant 42.26% grid energy consumption by the load and saving the costs by about RM123.3/day. To sum up, the notable contribution of this study is the proposed optimised FLC, whose robustness in controlling the charging–discharging of lithium-ion battery has been proven. Moreover, the optimised scheduling controller developed using BPSO schedules the operation of all MG sources, grids, fuzzy controlled ESS and loads in a 24 h duration to minimise the grid power demand and minimise the cost.

Declaration of competing interest

The authors declare that they have no known competing financial interests or personal relationships that could have appeared to influence the work reported in this paper.

Acknowledgement

References

Abdolrasol, M.G.M., Hannan, M.A., Mohamed, A., Amiruldin, U.A.U., Abidin, I.B.Z., Uddin, M.N., 2018. An optimal scheduling controller for virtual power plant and microgrid integration using the binary backtracking search algorithm. IEEE Trans. Ind. Appl. 54 (3), 2834–2844, https://doi.org/10.1109/TIA.2018.2797121.

Aghajani, G., Ghadimi, N., 2018. Multi-objective energy management in a micro-grid. Energy Rep. 4, 218–225, https://doi.org/10.1016/j.egyr.2017.10.002.

Alquthami, T., Ehsan, S., Faizan, M., 2020. Short-term optimal scheduling of hydro-thermal power plants using artificial bee colony algorithm. Energy Rep. 6, 984–992, https://doi.org/10.1016/j.egyr.2020.04.003.

Azzolini, I.A., Felice, V.Di, Fraboni, F., Cavallucci, L., Breschi, M., Rosa, A.D., Zini, G., 2018. Lead-acid battery modeling over full state of charge and discharge range. IEEE Trans. Power Syst. 33 (6), 6422–6429, https://doi.org/10.1109/TPWRS.2018.2850049.

Bhattacharjee, C., Roy, B.K., 2018. Fuzzy-supervisory control of a hybrid system to improve contractual grid support with fuzzy proportional – derivative and integral control for power quality improvement. IET Gener. Transmiss. Distrib. 12 (7), 1455–1465, https://doi.org/10.1049/iet-gtd.2017.0708.

Bhowmik, P., Chandak, S., Rout, P.K., 2018. State of charge and state of power management among the energy storage systems by the fuzzy tuned dynamic exponent and the dynamic PI controller. J. Energy Storage 19, 348–363, https://doi.org/10.1016/j.est.2018.08.004.

Bianchini, G., Casini, M., Pepe, D., Vicino, A., Zanvettor, G.G., 2019. An integrated model predictive control approach for optimal HVAC and energy storage operation in large-scale buildings. Appl. Energy 240, 327–340, https://doi.org/10.1016/j.apenergy.2019.01.187.

Chen, Y., Trifkovic, M., 2018. Optimal scheduling of a microgrid in a volatile electricity market environment : Portfolio optimization approach. Appl. Energy 226, 703–712, https://doi.org/10.1016/j.apenergy.2018.06.040.

Collotta, M., Pau, G., Maniscalco, V., 2017. A fuzzy logic approach by using particle swarm optimization for effective energy management in IWSNs. IEEE Trans. Ind. Electron. 64 (12), 9496–9506.

Faisal, M., Hannan, M.A., Ker, P.J., Hussain, A., Mansur, M., Blaabjerg, F., 2018. Review of energy storage system technologies in microgrid applications: Issues and challenges. IEEE Access 6 (1), https://doi.org/10.1109/ACCESS.2018.2841407.

Gao, D., Li, X., Chen, H., 2019. Application of improved particle swarm optimization in vehicle crashworthiness. Math. Probl. Eng. 2019, 1–10.

Geramifar, H., Shahabi, M., Barforoshi, T., 2017. Coordination of energy storage systems and DR resources for optimal scheduling of microgrids under uncertainties. IET Renew. Power Gener. 11 (2), 378–388, https://doi.org/10.1049/iet-rpg.2016.0094.

Ghasemi, A., Enayatzare, M., 2018. Optimal energy management of a renewable-based isolated microgrid with pumped-storage unit and demand response. Renew. Energy 123, 460–474, https://doi.org/10.1016/j.renene.2018.02.072.

Haddadian, H., Noroozian, R., 2017. Optimal operation of active distribution systems based on microgrid structure. Renew. Energy 104, 197–210, https://doi.org/10.1016/j.renene.2016.12.018.

Hajiaghasi, S., Salemnia, A., Hamzeh, M., 2019. Hybrid energy storage system for microgrids applications : A review. J. Energy Storage 21, 543–570, https://doi.org/10.1016/j.est.2018.12.017.

Hannan, M.A., Hoque, M., Peng, S.E., Uddin, M.N., 2017. Lithium-ion battery charge equalization algorithm for electric vehicle applications. IEEE Trans. Ind. Appl. 53 (1), 2541–2549, https://doi.org/10.1109/TIA.2017.2672674.

Hossain, A., Roy, H., Squartini, S., Fathi, A., 2019a. Modified PSO algorithm for real-time energy management in grid-connected microgrids. Renew. Energy 136, 746–757, https://doi.org/10.1016/j.renene.2019.01.005.

Hossain, A., Roy, H., Squartini, S., Zaman, F., Muttaqi, K.M., 2019b. Energy management of community microgrids considering degradation cost of battery. J. Energy Storage 22, 257–269, https://doi.org/10.1016/j.est.2018.12.021.

Keshtkar, A., Arzanpour, S., 2017. An adaptive fuzzy logic system for residential energy management in smart grid environments. Appl. Energy 186, 68–81, https://doi.org/10.1016/j.apenergy.2016.11.028.

Lai, C., Teh, J., Cheng, Y., Li, Y., 2017. A reflex-charging based bidirectional DC Charger for light electric vehicle and DC-microgrids. In: Proc. of the 2017 IEEE Region 10 Conference (TENCON), Malaysia, November 2017, 5-8, pp. 280–284.

Lalouni, S., Rekioua, D., Rekioua, T., Matagne, E., 2009. Fuzzy logic control of stand-alone photovoltaic system with battery storage. J. Power Sources 193, 899–907, https://doi.org/10.1016/j.jpowsour.2009.04.016.

Leonori, S., Paschero, M., Massimo, F., Mascioli, F., Rizzi, A., 2020. Optimization strategies for microgrid energy management systems by genetic algorithms. Appl. Soft Comput. J. 86, 105903, https://doi.org/10.1016/j.asoc.2019.105903.

Li, Y., Li, K., Xie, Y., Liu, J., Fu, C., Liu, B., 2020. Optimized charging of lithium-ion battery for electric vehicles: Adaptive multistage constant current–constant voltage charging strategy. Renew. Energy 146, 2688–2699, https://doi.org/10.1016/j.renene.2019.08.077.

Maleki, A., Nazari, M.A., Pourfayaz, F., 2020. Harmony search optimization for optimum sizing of hybrid solar schemes based on battery storage unit. Energy Rep. xxxx, https://doi.org/10.1016/j.egyr.2020.03.014.

Mallol-Poyato, R., Jiménez-Fernández, S., Díaz-Villar, P., Salcedo-Sanz, S., 2016. Adaptive nesting of evolutionary algorithms for the optimization of Microgrid's sizing and operation scheduling. Soft Comput. 21 (17), 4845–4857, https://doi.org/10.1007/s00500-016-2373-x.

Mansiri, K., Sukchai, S., Sirisamphanwong, C., 2018. Fuzzy control algorithm for battery storage and demand side power management for economic operation of the smart grid system at Naresuan University Thailand. IEEE Access 6, 32440–32449, https://doi.org/10.1109/ACCESS.2018.2838581.

Morstyn, T., Hredzak, B., Aguilera, R.P., Agelidis, V.G., 2018. Model predictive control for distributed microgrid battery energy storage systems. IEEE Trans. Control Syst. Technol. 26 (3), 1107–1114.

Motapon, S.N., Lupien-bedard, A., Dessaint, L., Fortin-blanchette, H., Al-haddad, K., 2017. A generic electrothermal li-ion battery model for rapid evaluation of cell temperature temporal evolution. IEEE Trans. Ind. Electron. 64 (2), 998–1008, https://doi.org/10.1109/TIE.2016.2618363.

Mukherjee, N., De, D., 2017. A new state-of-charge control derivation method for hybrid battery type integration. IEEE Trans. Energy Convers. 32 (3), 866–875.

Nemati, M., Braun, M., Tenbohlen, S., 2018. Optimization of unit commitment and economic dispatch in microgrids based on genetic algorithm and mixed integer linear programming. Appl. Energy 210, 944–963, https://doi.org/10.1016/j.apenergy.2017.07.007.

Nithyanandam, K., Barde, A., Lakeh, R.B., Wirz, R.E., 2018. Charge and discharge behavior of elemental sulfur in isochoric high temperature thermal energy storage systems. Appl. Energy 214, 166–177, https://doi.org/10.1016/j.apenergy.2017.12.121.

Perez, H.E., Hu, X., Dey, S., Moura, S.J., 2017. Optimal charging of Li-ion batteries with coupled electro-thermal-aging dynamics. IEEE Trans. Veh. Technol. 66 (9), 7761–7770.

Roslan, M.F., Hannan, M.A., Jern, P., Uddin, M.N., 2019. Microgrid control methods toward achieving sustainable energy management. Appl. Energy 240, 583–607, https://doi.org/10.1016/j.apenergy.2019.02.070.

Safari, S., Ardehali, M.M., Sirizi, M.J., 2013. Particle swarm optimization based fuzzy logic controller for autonomous green power energy system with hydrogen storage. Energy Convers. Manage. 65, 41–49, https://doi.org/10.1016/j.enconman.2012.08.012.

Salcedo-Sanz, S., Camacho-Gómez, C., Mallol-Poyato, R., Jiménez-Fernández, S., Ser, 2016. A novel coral reefs optimization algorithm with substrate layers for optimal battery scheduling optimization in micro-grids. Soft Comput. 20 (11), 4287–4300, https://doi.org/10.1007/s00500-016-2295-7.

Suresh, V., Muralidhar, M., Kiranmayi, R., 2020. Modelling and optimization of an off-grid hybrid renewable energy system for electrification in a rural areas. Energy Rep. 6, 594–604, https://doi.org/10.1016/j.egyr.2020.01.013.

Tang, R., Wang, S., 2019. Model predictive control for thermal energy storage and thermal comfort optimization of building demand response in smart grids. Appl. Energy 242, 873–882, https://doi.org/10.1016/j.apenergy.2019.03.038.

Tidjani, F.S., Hamadi, A., Chandra, A., Pillay, P., Ndtoungou, A., 2017. Optimization of standalone microgrid considering active damping technique and smart power management using fuzzy logic supervisor. IEEE Trans. Smart Grid 8 (1), 475–484, https://doi.org/10.1109/TSG.2016.2610971.

Too, J., Abdullah, A.R., Saad, N.M., 2019. A new co-evolution binary particle swarm optimization with multiple inertia weight strategy. Informatics 6 (21), 1–14.

Uzar, U., 2020. Political economy of renewable energy : Does institutional quality make a difference in renewable energy consumption? Renew. Energy 155, 591–603, https://doi.org/10.1016/j.renene.2020.03.172.

Vafamand, N., Khooban, M.H., Dragicevic, T., Blaabjerg, F., 2019. Networked fuzzy predictive control of power buffers for dynamic stabilization of DC microgrids. IEEE Trans. Ind. Electron. 66 (2), 1356–1362, https://doi.org/10.1109/TIE.2018.2826485.

Wang, S., Liu, Y., 2015. A PSO-based fuzzy-controlled searching for the optimal charge pattern of Li-ion batteries. IEEE Trans. Ind. Electron. 62 (5), 2983–2993, https://doi.org/10.1109/TIE.2014.2363049.

Wang, B., Xian, L., Manandhar, U., Ye, J., Zhang, X., Gooi, H.B., Ukil, A., 2019. Hybrid energy storage system using bidirectional single-inductor multiple-port converter with model predictive control in DC microgrids. Electr. Power Syst. Res. 173, 38–47, https://doi.org/10.1016/j.epsr.2019.03.015.

Yamchi, H.B., Shahsavari, H., Kalantari, N.T., Safari, A., Farrokhifar, M., 2019. A cost-efficient application of different battery energy storage technologies in microgrids considering load uncertainty. J. Energy Storage 22, 17–26, https://doi.org/10.1016/j.est.2019.01.023.

Zhang, F., Meng, K., Xu, Z., Dong, Z., Zhang, L., Wan, C., Liang, J., 2017. Battery ESS planning for wind smoothing via variable-interval reference modulation and self-adaptive SOC control strategy. IEEE Trans. Sustain. Energy 8 (2), 695–707, https://doi.org/10.1109/TSTE.2016.2615638.

Zhao, H., Wu, Q., Wang, C., Cheng, L., Rasmussen, C.N., 2015. Fuzzy logic based coordinated control of battery energy storage system and dispatchable distributed generation for microgrid. J. Modern Power Syst. Clean Energy 3 (3), 422–428, https://doi.org/10.1007/s40565-015-0119-x.

Zhu, W.H., Tatarchuk, B.J., 2016. Characterization of asymmetric ultracapacitors as hybrid pulse power devices for efficient energy storage and power delivery applications. Appl. Energy 169, 460–468, https://doi.org/10.1016/j.apenergy.2016.02.020.

Zhu, X., Xia, M., Chiang, H., 2018. Coordinated sectional droop charging control for EV aggregator enhancing frequency stability of microgrid with high penetration of renewable energy sources. Appl. Energy 210, 936–943, https://doi.org/10.1016/j.apenergy.2017.07.087.

Zolfaghari, M., Hosseinian, S.H., Fathi, S.H., Abedi, M., Gharehpetian, G.B., 2018. A new power management scheme for parallel-connected PV systems in microgrids. IEEE Trans. Sustain. Energy 9 (4), 1605–1617, https://doi.org/10.1109/TSTE.2018.2799972.